



Sub-Micron thick Step-Graded AlGa_N Buffer on Silicon with a High Buffer Breakdown Field

Elodie Carneiro, Stéphanie Rennesson, Sebastian Tamariz, Kathia Harrouche,
Fabrice Semond, Farid Medjdoub

► To cite this version:

Elodie Carneiro, Stéphanie Rennesson, Sebastian Tamariz, Kathia Harrouche, Fabrice Semond, et al..
Sub-Micron thick Step-Graded AlGa_N Buffer on Silicon with a High Buffer Breakdown Field. *physica
status solidi (a)*, 2023, 220 (16), pp.2200846. 10.1002/pssa.202200846 . hal-04042888

HAL Id: hal-04042888

<https://hal.science/hal-04042888>

Submitted on 23 Mar 2023

HAL is a multi-disciplinary open access archive for the deposit and dissemination of scientific research documents, whether they are published or not. The documents may come from teaching and research institutions in France or abroad, or from public or private research centers.

L'archive ouverte pluridisciplinaire **HAL**, est destinée au dépôt et à la diffusion de documents scientifiques de niveau recherche, publiés ou non, émanant des établissements d'enseignement et de recherche français ou étrangers, des laboratoires publics ou privés.

Sub-Micron thick Step-Graded AlGa_N Buffer on Silicon with a High Buffer Breakdown Field

Elodie Carneiro, Stéphanie Rennesson, Sebastian Tamariz, Kathia Harrouche, Fabrice Semond and Farid Medjdoub*

E. Carneiro, K. Harrouche, F. Medjdoub

CNRS-IEMN, Institute of Electronics, Microelectronics and Nanotechnology, Av. Poincare, 59650 Villeneuve d'Ascq, France

E-mail: elodie.carneiro@iemn.fr

E. Carneiro, S. Rennesson, S. Tamariz

EasyGaN SAS, Rue Bernard Grégory 06905 Sophia Antipolis, France

S. Tamariz, F. Semond

Université Côte d'Azur, CNRS, CRHEA, rue Bernard Grégory, 06905 Sophia Antipolis, France

Keywords: GaN-on-Si, HEMT, MBE, buffer breakdown, Load-Pull, PAE, P_{OUT}, 10 GHz

We report on a sub-micron thick AlGa_N/Ga_N high electron mobility transistor (HEMT) epilayers grown on silicon substrate with a state-of-the art vertical buffer breakdown field as high as 6 MV/cm enabling a high transistor breakdown voltage of 250 V for short gate to drain distances despite such a thin structure. HEMTs with a gate length of 100 nm exhibit good DC characteristics with a low drain-induced barrier lowering as low as 100 mV/V for a V_{DS} of 30 V. Breakdown voltages of each epilayer from the decomposed heterostructure reveals that the outstanding breakdown strength is attributed to the insertion of Al-rich AlGa_N in the buffer layers combined with an optimized AlN nucleation layer. As a result, large signal measurements at 10 GHz could be reliably achieved up to V_{DS} = 35 V despite the use of a 100 nm gate length. These results demonstrate the potential of sub-micron thick buffer GaN-on-Si heterostructures for high frequency applications.

1. Introduction

This article has been accepted for publication and undergone full peer review but has not been through the copyediting, typesetting, pagination and proofreading process, which may lead to differences between this version and the [Version of Record](https://onlinelibrary.wiley.com/doi/10.1002/pssa.202200846). Please cite this article as [doi: 10.1002/pssa.202200846](https://onlinelibrary.wiley.com/doi/10.1002/pssa.202200846).

GaN-based High Electron Mobility Transistors (HEMTs) are being extensively used for high power millimeter-wave applications owing to their outstanding properties such as high thermal and chemical stability, high breakdown field (3.3 MV/cm), and high electron saturation velocity (2.5×10^7 cm/s) resulting in superior performances.^[1,2] Because of the large lattice and thermal expansion coefficient mismatch between GaN and silicon carbide (SiC), silicon (Si) or sapphire substrates, GaN HEMTs are typically grown with thick buffer layers (several μm) to minimize growth defects/dislocations at the vicinity of the 2DEG.^[3-6] However, a thick buffer degrades the thermal dissipation and increases the epi-wafer cost. Some recent reports have demonstrated promising DC and RF performances of AlGaIn/GaN HEMTs grown on SiC with a total thickness lower than 1 μm .^[7,8] However, the large thermal expansion coefficient difference makes the growth on Si substrates even more challenging, thus, high performance with sub-micron thick GaN HEMTs have not been proven yet to our knowledge.^[9-13] Moreover, although AlGaIn/GaN HEMT is the most mature technology, which demonstrated outstanding power performances in the microwave range, the device downscaling for higher frequency of operation generally results in a reduced breakdown voltage degrading the overall device performances.^[14-18] In this work, we demonstrate the possibility to achieve a high vertical buffer breakdown field in a submicron thick epi-stack. The high breakdown field is understood to originate from the use of Al-rich AlGaIn buffer layers and a high quality AlN nucleation layer. Furthermore, large signal performances at 10 GHz have been carried out on short devices with a gate length of 100 nm. The results show the potential of this thin AlGaIn/GaN-on-Si heterostructure for high frequency applications.

2. Experimental Details

Figure 1 shows the cross section of the HEMT structures. Two different AlN nucleation layer (NL) with thickness 1 (t_1) lower than 100 nm and thickness 2 (t_2) between 100 and 300 nm have been grown by ammonia-assisted Molecular Beam Epitaxy (NH_3 -MBE) on highly-resistive Si(111) substrates ($\rho > 5$ k Ω .cm) using a RIBER MBE49 growth reactor. The structure is then followed by three step-graded $\text{Al}_x\text{Ga}_{1-x}\text{N}$ buffer layers ($\text{Al}_{0.60}\text{Ga}_{0.40}\text{N}$ / $\text{Al}_{0.30}\text{Ga}_{0.70}\text{N}$ / $\text{Al}_{0.08}\text{Ga}_{0.92}\text{N}$), a 150 nm thick GaN channel layer, a 1 nm thick AlN spacer and a 14 nm thick $\text{Al}_{0.32}\text{Ga}_{0.68}\text{N}$ barrier. Finally, the structure was capped with a GaN layer. The total stack thickness is less than 650 nm for the structure with AlN NL t_1 and the second structure has also a total thickness below 1 μm . The step-graded $\text{Al}_x\text{Ga}_{1-x}\text{N}$ buffer is used both to enhance the electron confinement and the breakdown voltage by increasing the overall bandgap. Device processing started with the formation of the source and drain ohmic contacts by partially etching the AlGaIn barrier layer with BCl_3/SF_6 plasma in an Inductively Coupled Plasma (ICP) reactor prior to the metallization. A Ti/Al/Ni/Au metal stack was deposited

and annealed at 800 °C. The devices were isolated using Nitrogen implantation. Then, Ni/Au gates of 3 μm length were defined by optical lithography. Finally, the devices were passivated with 200 nm plasma enhanced chemical vapor deposition (PECVD) Si_3N_4 prior to the Ti/Au pads deposition enabling electrical measurements. The two-dimensional electron gas (2DEG) properties have been extracted at room temperature by Hall effect measurements and showed a charge density of $1.1 \times 10^{13} \text{ cm}^{-2}$ and $1.3 \times 10^{13} \text{ cm}^{-2}$ with an electron mobility of $1050 \text{ cm}^2/\text{V.s}$ and $1530 \text{ cm}^2/\text{V.s}$ for AlN NL t_1 and t_2 , respectively. The AlN NL thickness indirectly impacts the electron mobility. Indeed, when increasing the thickness of the AlN, the crystalline quality is improved (with less dislocations and larger grains). In addition, the step-graded $\text{Al}_x\text{Ga}_{1-x}\text{N}$ buffer layers on top and the GaN channel layer are more compressed, which lead to an overall better crystalline quality, resulting in an increased electron mobility of the 2DEG.

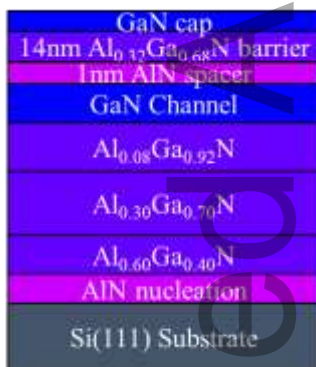


Figure 1. Schematic cross section of the sub-micron thick AlGaN/GaN HEMT heterostructures grown on Si(111) using a step-graded $\text{Al}_x\text{Ga}_{1-x}\text{N}$ buffer layers.

3. DC and Breakdown Characteristics

Vertical breakdown voltage measurements with a grounded substrate and isolated ohmic contacts on the front side have been performed using a Keysight B1505A high-voltage parameter analyzer. **Figure 2** shows typical vertical leakage characteristics of the heterostructures at room temperature measured on several locations across the samples.

Despite the sub-micron thick epi-stack, the leakage current distribution is rather uniform showing that a thick buffer is not mandatory to maintain a high material quality close to the 2DEG. It can also be noticed that a leakage current below $1 \text{ mA}/\text{cm}^2$ is observed up to 400 V with a hard breakdown voltage of 500 V for AlN NL t_1 . This results in a remarkable vertical breakdown field higher than 6 MV/cm (calculated by normalizing the hard breakdown voltage with the total epi-stack thickness), which is significantly higher than the theoretical value of 3 MV/cm for GaN and close to the

theoretical value of AlN. On the other hand, it can be pointed out that an AlN NL t_2 thicker than t_1 using the same epi-stack results in a much larger leakage current (**Figure 2**).

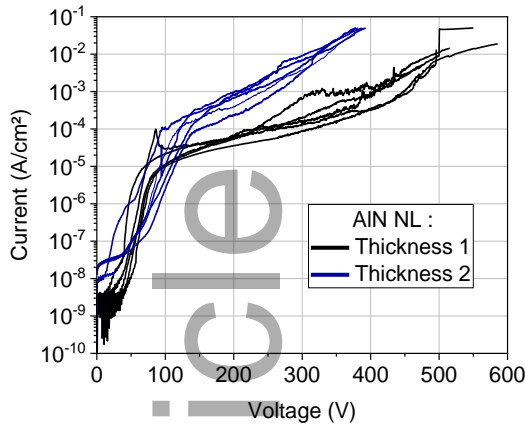


Figure 2. Vertical breakdown characteristics of the sub-micron thick GaN-on-Si HEMTs with AlN NL t_1 and t_2 .

To better understand the origin of this result, we performed a decomposition study of the structure with AlN NL t_1 by etching several samples down to the different epilayers: GaN channel, $\text{Al}_{0.08}\text{Ga}_{0.92}\text{N}$, $\text{Al}_{0.30}\text{Ga}_{0.70}\text{N}$, $\text{Al}_{0.60}\text{Ga}_{0.40}\text{N}$ and Si substrate (**Figure 3**). The structure was first etched until the substrate, which shows a vertical breakdown voltage lower than 100 V. For all the other samples, this value was subtracted in order to remove the electrical contribution of the substrate on the vertical breakdown voltage. The vertical breakdown voltage of the different decomposed structures shows that the remarkable breakdown field is clearly attributed to the insertion of Al-rich AlGaN into the buffer layers combined with an optimized AlN NL offering outstanding breakdown strength of about 15 MV/cm, close to the theoretical value of AlN.^[19]

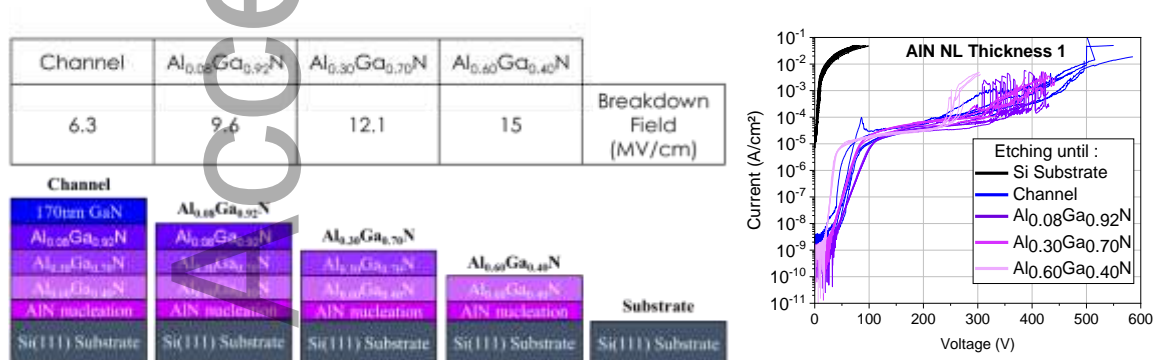


Figure 3. Vertical breakdown voltage and breakdown field characteristics of the decomposed step-graded $\text{Al}_x\text{Ga}_{1-x}\text{N}$ buffer and the Si(111) substrate.

The three-terminal off-state breakdown voltage has been measured at gate source voltage (V_{GS}) -6 V for various gate to drain distance varying from $5\text{ }\mu\text{m}$ to $40\text{ }\mu\text{m}$ and for AlN NL t_1 and t_2 as shown in

Figure 4. It can be noticed that a drain leakage current (I_D) well below 100 $\mu\text{A}/\text{mm}$ up to drain source voltage (V_{DS}) 200 V is observed regardless of the device design for AlN NL t_1 (see **Figure 4**) while the AlN NL t_2 transistors deliver two orders of magnitude larger leakage current even at lower bias (see **Figure 4**). For both thicknesses, the transistor breakdown voltage of about 250 V is independent of the gate to drain distance due to the thin heterostructure.

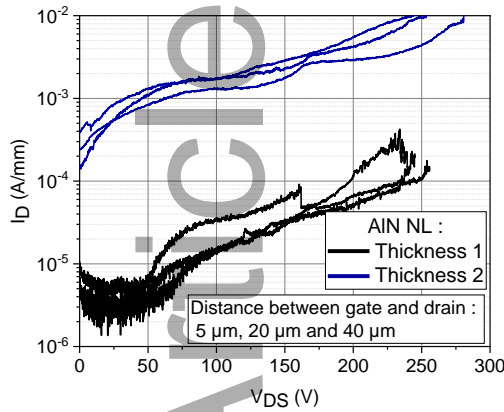


Figure 4. Three-terminal off-state breakdown voltage characteristics of sub-micron thick $2 \times 50 \mu\text{m}$ AlGaIn/GaN HEMTs with AlN NL t_1 and t_2 for various gate to drain distances.

In order to assess the full potential of the structure with an AlN NL t_1 the structure was reproduced and capped with an *in situ* SiN passivation layer to efficiently passivate the surface states. To increase the electric field below the gate a similar fabrication process was used, with this time Ni/Au T-gates defined by e-beam lithography allowing the formation of 100 nm gate lengths (L_G). DC measurements have been carried out on the structure with an AlN NL t_1 using a Keysight A2902A static modular and source monitor. **Figure 5** shows typical output and transfer characteristics of $2 \times 50 \mu\text{m}$ transistors with L_G of 100 nm and a gate-to-drain distance (L_{GD}) of 0.5 μm . The gate source voltage was swept from -6 to $+2$ V with a step size of 1 V. A low maximum drain current $I_{D,\text{max}}$ of about 0.74 A/mm has been measured due to the low 2DEG mobility of this structure (**Figure 5.a**). A pinch-off voltage $V_{TH} = -3.9$ V (shown in **Figure 5.b**) is observed with a drain leakage current lower than 1 $\mu\text{A}/\text{mm}$. **Figure 5.b** displays the transfer characteristics with a compliance fixed at 150 mA/mm and swept from $V_{DS} = 2$ to 30 V using a step of 1 V. A low threshold voltage shift as a function of V_{DS} is observed under high electric field up to 30 V, which confirms a proper electron confinement within the 2DEG of the sub-micron step-graded $\text{Al}_x\text{Ga}_{1-x}\text{N}$ buffer reflected by a low drain-induced barrier lowering (DIBL) of 100 mV/mm. A transconductance (G_m) of 200 mS/mm has been measured (**Figure 5.c**). However, this value can be significantly increased by reducing the access resistances. Currently, the contact resistances are as high as 0.6 $\Omega\cdot\text{mm}$, as extracted by transmission line measurements. Pulsed I_D - V_{DS} characteristics revealing the charge trapping effects when using various

quiescent bias points are depicted in **Figure 5.d**. The open channel DC pulsed measurements are shown at $V_{GS} = +2$ V with various quiescent drain voltages at room temperature. The specific pulsed I–V protocol based on I–V characteristics has been settled with the following quiescent bias points: cold point at ($V_{GQ} = 0$ V, $V_{DQ} = 0$ V), gate lag at ($V_{GQ} = -4$ V, $V_{DQ} = 0$ V) and drain lag at ($V_{GQ} = -4$ V, $V_{DQ} = 10, 15$ and 20 V) using a pulse width of $1 \mu\text{s}$ and a duty cycle of 1% . $2 \times 50 \mu\text{m}$ transistors with L_{GD} of $0.5 \mu\text{m}$ and L_G of 100 nm reveal low charge trapping effects as shown from the pulsed I_D – V_{DS} characteristics. Secondary-ion mass spectrometry (SIMS) of the sub-micron thick GaN-on-Si HEMTs with AlN NL t_1 reveal unintentional carbon and oxygen doping in the structure. The carbon concentration is in the range of $1\text{--}5 \times 10^{15}$ atoms/ cm^3 in the step-graded $\text{Al}_x\text{Ga}_{1-x}\text{N}$ buffer layers as well as in the GaN channel; while the oxygen concentration is lower than 1×10^{17} atoms/ cm^3 in the buffer. This reduced unintentional carbon doping is considered low enough to avoid buffer trapping effects.^[20] The combination of a low carbon doping concentration in the buffer, a surface passivation with *in situ* SiN and an optimized fabrication process leads to low charge trapping effects.

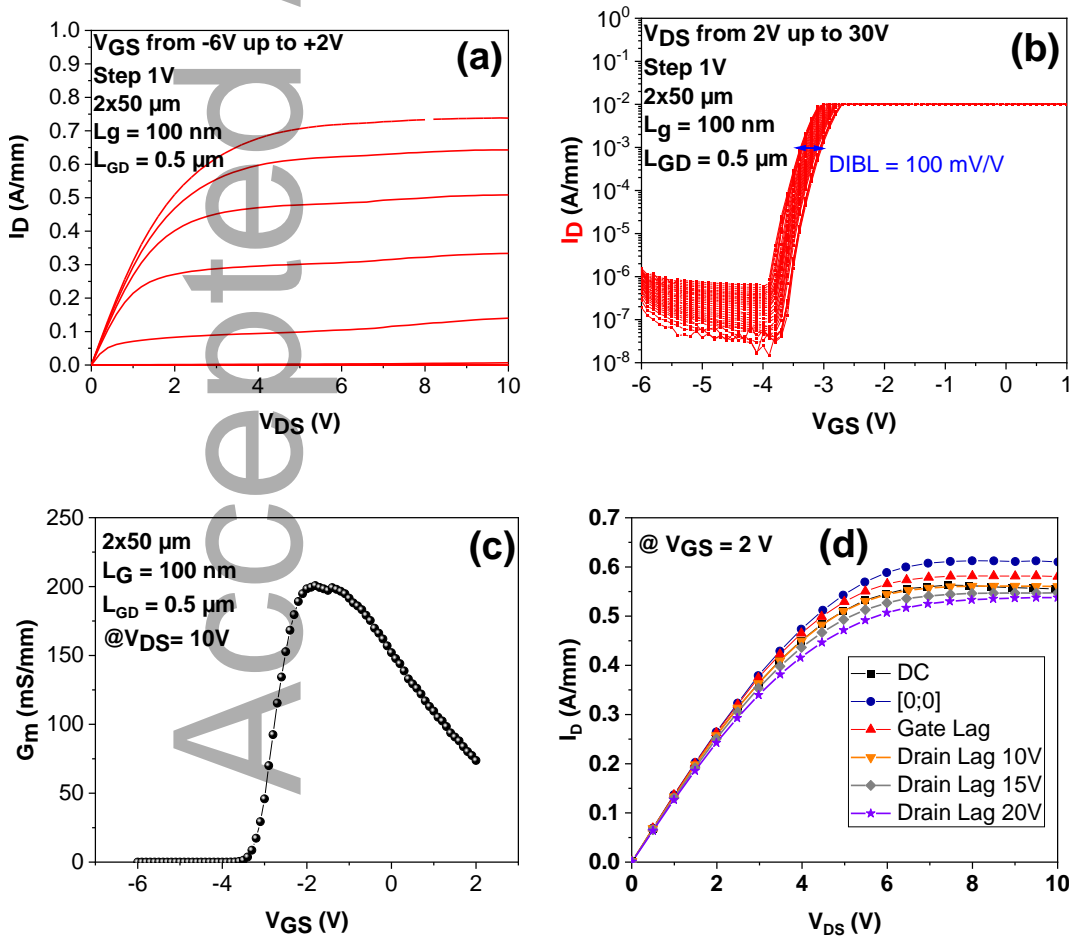
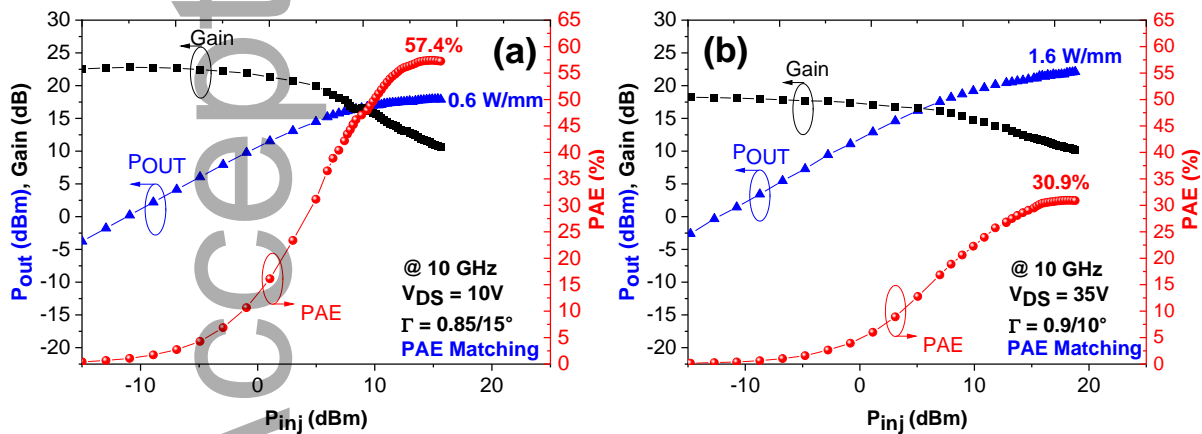


Figure 5. (a) Output characteristics, (b) transfer characteristics, (c) transconductance and (d) open channel pulsed I_D – V_{DS} output characteristics of a sub-micron thick $2 \times 50 \mu\text{m}$ AlGaIn/GaN HEMT with AlN NL t_1 , $L_{GD} = 0.5 \mu\text{m}$ and $L_G = 100 \text{ nm}$.

This article is protected by copyright. All rights reserved

4. 10 GHz Large Signal Characteristics

Large signal characterizations have been carried out at 10 GHz on a nonlinear vector network analyzer system (Keysight Network Analyser: PNA-X, N5245A-NVNA) capable of on-wafer large signal device characterization up to the Q-band in continuous and pulsed mode. Further details of the power bench can be found in.^[21] **Figures 6.a** and **Figure 6.b** show power performances of $2 \times 50 \mu\text{m}$ transistor with $L_{\text{GD}} = 0.5 \mu\text{m}$ and $L_{\text{G}} = 100 \text{ nm}$ at $V_{\text{DS}} = 10 \text{ V}$ and 35 V , respectively. A saturated output power density (P_{OUT}) of 0.6 W/mm associated to a power added efficiency (PAE) of 57.4% at $V_{\text{DS}} = 10 \text{ V}$ is measured. For $V_{\text{DS}} = 35 \text{ V}$, a P_{OUT} of 1.6 W/mm associated to a PAE of 30.9% has been achieved. Moreover, after many Load-Pull sweeps, no degradation of the devices is observed up to $V_{\text{DS}} = 35 \text{ V}$ as seen in **Figure 6.c**. This proves that this heterostructure enables high voltage operation without degradation despite the use of a gate length as short as 100 nm . The promising robustness is attributed to the high quality of the sub-micron thick step-graded $\text{Al}_x\text{Ga}_{1-x}\text{N}$ buffer layers. The rather limited output power density is explained by the low maximum drain current of this structure, which depends on the electron mobility that needs to be further enhanced. Finally, the drop of the PAE between $V_{\text{DS}} = 10 \text{ V}$ and 35 V is attributed to the poor thermal dissipation of the Si substrate. Therefore, further optimization of the structure, together with substrate thinning and use of a heat sink will significantly enhance the device's performance.



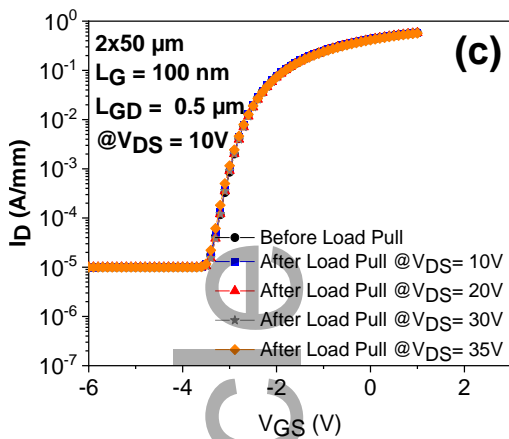


Figure 6. Large signal performances at 10 GHz for a $2 \times 50 \mu\text{m}$ transistor with $L_{\text{GD}} = 0.5 \mu\text{m}$ and $L_{\text{G}} = 100 \text{ nm}$ at (a) $V_{\text{DS}} = 10 \text{ V}$, (b) $V_{\text{DS}} = 35 \text{ V}$. (c) Transfer characteristics after more than 40 Load Pull sweep up to $V_{\text{DS}} = 35 \text{ V}$.

6. Conclusion

In this work, we investigated sub-micron thick AlGaIn/GaN HEMTs grown on Si(111) substrates for high frequency applications. This MBE grown heterostructure, with a buffer thickness below 650 nm including Al-rich step-graded layers, shows promising features such as an outstanding vertical breakdown field higher than 6 MV/cm. DC characteristics reveal fully functional transistors with low off-state leakage current under high electric field up to 30 V despite a short gate length of 100 nm. This technology enables to operate the transistors under high drain bias at high frequency with enhanced robustness. This achievement is attributed to the optimization of the sub-micron thick step-graded $\text{Al}_x\text{Ga}_{1-x}\text{N}$ buffer layer combined with an optimized AlN nucleation layer enabling a high electron confinement under high electric field.

Acknowledgements

This work was supported by the French RENATECH network, and the French National grant GaNeXT ANR-11-LABX-0014. S. Tamariz thanks ANR and CNRS for the implementation of the “Plan de Relance – Préservation de l’emploi R&D” program ANR-21-PRRD-0001-01.

Received: ((will be filled in by the editorial staff))

Revised: ((will be filled in by the editorial staff))

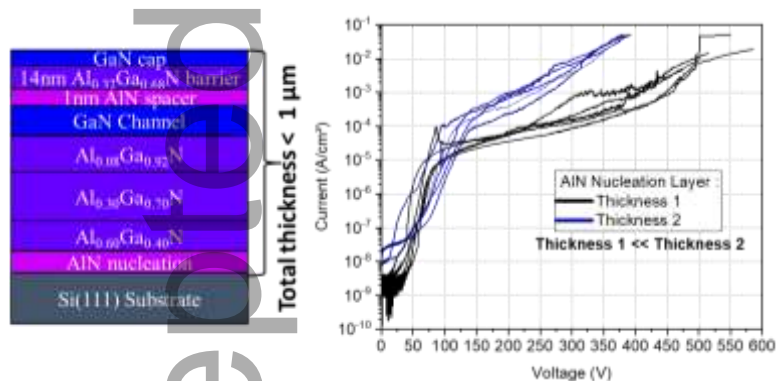
Published online: ((will be filled in by the editorial staff))

References

This article is protected by copyright. All rights reserved

- [1] U.K. Mishra, P. Parikh, Y.F. Wu, *Proceedings of the IEEE*, **2002**, 90, 1021567.
- [2] K. Harrouche, R. Kabouche, E. Okada, F. Medjdoub, *IEEE Journal of the Electron Devices Society*, **2019**, 7, 2952314.
- [3] W. Liu, B. Romanczyk, M. Guidry, N. Hatui, C. Wurm, W. Li, P. Shrestha, X. Zheng, S. Keller, U.K. Mishra, *IEEE Microwave and Wireless Components Letters*, **2021**, 31, 3067228.
- [4] J.S. Moon, R. Grabar, J. Wong, M. Antcliffe, P. Chen, E. Arkun, I. Khalaf, A. Corrion, J. Chappell, N. Venkatesan, P. Fay, *Electron Lett.*, **2020**, 56, 0281.
- [5] K. Makiyama, S. Ozaki, T. Ohki, N. Okamoto, Y. Minoura, Y. Niida, Y. Kamada, K. Joshin, K. Watanabe, Y. Miyamoto, *IEEE International Electron Devices Meeting (IEDM)*, **2015**, 7409659.
- [6] K. Harrouche, R. Kabouche, E. Okada, F. Medjdoub, *IEEE/MTT-S International Microwave Symposium Digest (IMS)*, **2020**, 9223971.
- [7] D.Y. Chen, A. Malmros, M. Thorsell, H. Hjelmgren, O. Kordina, J.T. Chen, N. Rorsman, *IEEE Electron Device Letters*, **2020**, 41, 2988074.
- [8] D.Y. Chen, K.H. Wen, M. Thorsell, M. Lorenzini, H. Hjelmgren, J.T. Chen, N. Rorsman, *Physica Status Solidi (A) Applications and Materials Science*, **2022**, 202200496.
- [9] K.J. Chen, O. Haberen, A. Lidow, C.L. Tsai, T. Ueda, Y. Uemoto, Y. Wu, *IEEE Trans Electron Devices*, **2017**, 64, 2657579.
- [10] Y. Cordier, F. Semond, P. Lorenzini, N. Grandjean, F. Natali, B. Damilano, J. Massies, V. Hoël, A. Minko, N. Vellas, C. Gaquière, J.C. DeJaeger, B. Dessertene, S. Cassette, M. Surrugue, D. Adam, J.-C. Grattapain, S.L. Delage, *Physica Status Solidi (C)*, **2002**, 200390117.
- [11] P. Altuntas, F. Lecourt, A. Cutivet, N. Defrance, E. Okada, M. Lesecq, S. Rennesson, A. Agboton, Y. Cordier, V. Hoel, J.C. de Jaeger, *IEEE Electron Device Letters*, **2015**, 36, 2404358.
- [12] D. Marcon, J. Viaene, F. Vanaverbeke, X. Kang, S. Lenci, S. Stoffels, R. Venegas, P. Srivastava and S. Decoutere, *2012 7th European Microwave Integrated Circuit Conference*, **2012**, pp. 325-328.
- [13] F. Medjdoub, M. Zegaoui, B. Grimbart, D. Ducatteau, N. Rolland, P.A. Rolland, *IEEE Electron Device Letters*, **2012**, 33, 2198192.
- [14] M. Borga, M. Meneghini, D. Benazzi, E. Canato, R. Püsche, J. Derluyn, I. Abid, F. Medjdoub, G. Meneghesso, E. Zanoni, *Microelectronics Reliability*, **2019**, 100-101, 113461.
- [15] S. Moench, S. Müller, R. Reiner, P. Waltereit, H. Czap, M. Basler, J. Hüchelheim, L. Kirste, I. Kallfass, R. Quay, O. Ambacher, *Physica Status Solidi (A) Applications and Materials Science*, **2021**, 218, 202000404.

- [16] N. Remesh, N. Mohan, S. Raghavan, R. Muralidharan, D.N. Nath, *IEEE Trans Electron Devices*, **2020**, 67, 2989421.
- [17] X. Yu, J. Ni, Z. Li, J. Zhou, C. Kong, *Jpn J Appl Phys.*, **2014**, 53, 051001.
- [18] M. Borga, M. Meneghini, I. Rossetto, S. Stoffels, N. Posthuma, M. van Hove, D. Marcon, S. Decoutere, G. Meneghesso, E. Zanoni, *IEEE Trans Electron Devices*, **2017**, 64, 2726440.
- [19] R.J. Kaplar, A.A. Allerman, A.M. Armstrong, M.H. Crawford, J.R. Dickerson, A.J. Fischer, A.G. Baca, E.A. Douglas, *ECS Journal of Solid State Science and Technology*, **2017**, 6, 0111702.
- [20] K. Harrouche, S. Venkatachalam, F. Grandpierron, E. Okada, F. Medjdoub, *Applied Physics Express*, **2022**, 15, 116504.
- [21] R. Kabouche, E. Okada, E. Dogmus, A. Linge, M. Zegaoui, F. Medjdoub, *IEEE Microwave and Wireless Components Letters*, **2017**, 27, 2678424.



A sub-micron thick step-graded AlGa_N buffer is grown on Si by ammonia-Molecular Beam Epitaxy (NH₃-MBE). An outstanding vertical buffer breakdown field of 6 MV/cm is demonstrated. Moreover, DC and large signal characteristics for 100 nm gate length shows high electron confinement under high electric field enabling operation under high drain bias at high frequency with high robustness.